CALCULATION OF REMAINING MOBILE OIL, DUNE FIELD, UNIVERSITY LANDS, CRANE COUNTY, TEXAS[1]

F. J. Lucia, D. G. Bebout, C. R. Hocott, G. E. Fogg, and G. W. Vander Stoep
Bureau of Economic Geology
The University of Texas at Austin

INTRODUCTION

A significant available resource of unrecovered mobile oil resides within Grayburg reservoirs as a result of low ultimate recoveries of less than 30 percent of the large estimated volume of original oil in place. This low ultimate recovery from conventional primary and secondary recovery methods is due mainly to the heterogeneity typical of these reservoirs. Evidence of this heterogeneity is well displayed in the Dune field by significant production inequalities, particularly within the Mobil University Unit 15/16. The cumulative production from Section 15 is about 10 million barrels, whereas that from Section 16 is only 2 million barrels. This difference between the two adjacent sections cannot be attributed solely to varying production practices, but rather to major changes in rock fabric and depositional facies. Within Section 15, wells from the same reservoir have yielded widely varying amounts of total production, further demonstrating even smaller scale heterogeneity.

The fraction of original oil in place that can be produced from a reservoir depends on the natural reservoir drive mechanism and the supplementary recovery methods used. The natural reservoir drive mechanism in the Dune field is solution gas drive; recovery factors from this type of drive are normally less the 30 percent. Water flooding is the supplementary recovery method employed in the Dune field. The recovery factor of this method depends on the volume of reservoir rock contacted by water. Some of the oil cannot be removed even by waterflooding due to capillary forces. This oil is residual oil. The balance of the oil in the reservoir is mobile oil. As oil is produced, the volume of mobile oil is reduced, and the mobile oil left in the reservoir is the remaining mobile oil. This remaining volume is simply the original oil in place expressed as stock-tank oil under surface conditions (STOOIP) less the sum of the volume of oil produced and the volume of residual oil at surface conditions.

The distribution of remaining mobile oil can be determined by mapping the original oil in place, the volume of oil produced, and the residual-oil saturation. The original oil in place and the volume of oil produced will be a function of the distribution of porosity, permeability, and the capillary forces, which are in turn a function of the geologic processes that formed the reservoir rock. The

---

1 Publication authorized by the Director, Bureau of Economic Geology, The University of Texas at Austin.

distributions of porosity, permeability, and water saturation in Section 15 of the Dune field are described by integrating inferred geologic processes, core and thin-section interpretations, results of core analyses, wireline log interpretation, and production data.

FIELD GEOLOGY

The Dune field is located on the eastern edge of the Central Basin Platform of the Permian Basin (Fig. 1). It produces from the Grayburg Formation of Guadalupian (Permian) age. The Grayburg represents a transition from the abundant siltstone, anhydritic dolomite, and anhydrite of the overlying Queen Formation to the dolomite of the underlying San Andres Formation. On the basis of the study of Dune field cores, the Grayburg Formation is divided into three units (Fig. 2, Fig. 3). The lower unit is 80 to 140 ft thick and extends from the top of the San Andres to the M log marker. It is typically a fusulinid wackestone with fusulinid-mold porosity but very low matrix porosity. The middle unit extends from the M marker up to the base of the A siltstone marker and is about 100 ft thick. A vertically structured facies is present in the western sector of Mobil Unit 15/16, changing to a crinoid packstone/grainstone facies in the eastern sector. Porosity is best developed in the grainstone beds. The upper unit, which is defined from the top of the A siltstone marker up to the base of the "Brown Lime", constitutes a single upward-shoaling, progradational cycle. Form bottom to top, the sequence consists of fusulinid wackestone at the base, pellet and ooid grainstone near the top, and pisolite grainstone and anhydrite at the top. Several siltstone beds occur throughout the unit and are used as zonal boundaries.

The Dune field lies on the northeast side of a low-relief structure that dips gently to the northeast into the Midland Basin. The highest part of the structure is just to the west of the Dune field where the top of the Grayburg Formation lies less than 300 ft below sea level. Mobil University Unit 15/16 is located on the east side of the structure. The dip of the structure steepens considerably farther to the east of Section 15, and in less than 1 mi the top of the Grayburg Formation is at 1,300 ft below sea level.

Dune field includes a total oil column of about 800 ft and a small 50- to 100-ft-thick gas column at the top of the structure on the west side of the field (Fig. 4). The top seal for the Dune field reservoir comprises nonporous supratidal anhydrite-cemented carbonates and anhydrite. Oil occurs locally in a few vugs in this generally nonporous facies, but no significant volume of hydrocarbons has been found. The subtidal reservoir facies of the Grayburg thin updip to the west and also are systematically replaced by nonproductive supratidal facies. At the west edge of the field only 100 ft of low-porosity nonproductive subtidal dolostone remains. The resulting low-porosity subtidal zone marks the west edge of Dune field development. The bottom seal is formed by nonporous supratidal sediments that cap the underlying upward-shallowing cycle of the San Andres Formation. Limited data indicate that this supratidal unit thins eastward toward the Midland Basin and wedges out near the east side of the Dune field. The free-water table probably coincides with

the subsea depth marked by the termination of the bottom seal. The deepest productive perforations in the field are along the east edge and are consistent with the projected subsea depth of the bottom seal and the free-water table.

ORIGINAL OIL IN PLACE

The stock-tank original volume of oil in place (STOOIP) is calculated from the volumetric equation using a formation volume factor of 1.128. STOOIP calculations require accurate values of porosity and water saturation. These values are obtained from wireline logs and core analyses, which are quite accurate for most carbonates. However, the Dune field contains significant amounts of gypsum, a mineral that can have a large effect on the accuracy of porosity values obtained from wireline logs and core analyses.

Gypsum Effects

Gypsum ($CaSO_4*2H_2O$) is the hydrated form of anhydrite ($CaSO_4$). The bound water is released above a temperature of 60° C, and the mineral alters either to anhydrite (which is anhydrous) or to the hemihydrate form, bassanite ($CaSO_4*1/2H_2O$) (Tilly and others, 1981). The loss of bound water from gypsum also increases the density. Gypsum has a density of 2.35, bassanite 2.70, and anhydrite 2.95. This increase in density is accompanied by a decrease in grain volume, which results in increased porosity. Since permeability is also directly related to porosity, an increase in permeability results as well.

Routine core analysis uses temperatures higher than 60° C, and bound water from gypsum is released, resulting in erroneously high porosity and permeability values. Special low-temperature core analysis procedures have been developed that minimize the loss of bound water from gypsum. Only cores analyzed by this special low-temperature technique were used in this study.

Gypsum has a large effect on neutron- and density-log responses and little effect on acoustic-log response. The neutron log measures the hydrogen ion content of the rock and converts those measurements to porosity (ϕ_n), assuming that all the hydrogen ions are in the fluids. Hydrogen ions in the bound water of gypsum are recorded as porosity on the neutron log, producing a large error in porosity calculations if large volumes of gypsum are present.

The effect of gypsum on neutron, density, and acoustic logs is shown by the following equations. The neutron log is affected most, and the acoustic log the least.

$$\phi_n = 1.0\phi + 0.0C + 0.02D + 0.0A + 0.49G - 0.04Q \quad (1)$$

$$\rho_b = 1.10\phi + 2.71C + 2.84D + 2.98A + 2.35\ G + 2.65Q \quad (2)$$

$$\Delta t = 185\phi + 45C + 42D + 50A + 53G + 55Q \quad (3)$$

Where ϕ_n, ρ_b, and Δt are input values from neutron, density, and acoustic logs, respectively, ϕ is fractional porosity, and C, D, A, G, and Q are the fractions of bulk volume attributed to calcite, dolomite, anhydrite, gypsum, and quartz, respectively.

Theoretically, the porosity of a formation composed of dolomite, anhydrite, and gypsum can be calculated using three porosity logs, the above three equations, and the identity equation, which states that the mineral volumes plus the pore volume must equal one (Pirson, 1983). This procedure was tested using mineralogic data from well 1559, and the resulting mineral percentages were significantly different from those obtained from X-ray diffraction and thin-section description. Porosity values could not be compared because the core was analyzed using high temperatures. Since the calculated mineral percentages are in error, the porosity values are also considered to be in error. Because the acoustic log is the least affected by the presence of gypsum, it is used as the porosity tool in this study.

Correlation of Acoustic-Log Response and Core Porosity

The correlation between transit time (Δt), as measured by the acoustic log, and core porosity was investigated in four wells, Mobil University Nos. 1535, 1539, 1540, and 1560. Acoustic logs do not measure all the vuggy porosity, but detailed studies of cores from this field have shown very little vuggy porosity (Fig. 5). Beds containing more than 30 percent quartz siltstone, (the A, B, C, Y, and Z siltstones) were excluded from this analysis because the presence of quartz significantly changes the relationship between transit time and porosity.

In order to calibrate transit time with core porosity, the two sets of data must be normalized both for depth and sampling interval. Depths from the core analysis report were initially adjusted to log depths by comparing gamma-ray logs of cores with wireline gamma-ray logs. For well 1560, this procedure resulted in a correlation of only 0.67 between core porosity and transit time (Fig. 6A). Because the acoustic log presents data averaged over a few feet, 3-ft running averages where made of the core-porosity data. A plot of those values against transit time resulted in an increase in the correlation to 0.78 (Fig. 6B). A plot of transit time and 3-ft averaged core porosity against depth showed that the core-porosity curve was displaced in some areas by 1 to 2 ft relative to the transit-time curve. This displacement is attributed to inaccurate core depth due to missing core or to incorrect depth corrections made while logging the interval. The porosity curve was shifted to match the transit-time curve, which in well 1560 improved the correlation to 0.86 (Fig. 6C).

The intercept transit time (Δt where porosity = 0) should be the transit time for the composite rock, which in the Dune field is composed primarily of dolomite, anhydrite, and gypsum. The transit time for pure dolomite is 43.5 microseconds; however, anhydrite and gypsum have transit times of approximately 50 and 53 microseconds, respectively.

Using the results of low-temperature analysis, transit-time - core-porosity curves for wells 1535 and 1560 were prepared. The resulting intercept transit-time values are 46.8 and 49.0 microseconds, reflecting a mixture of dolomite and sulfate minerals.

Both high- and low-temperature analyses were performed on wells 1535 and 1560. As shown above, the low-temperature data give expected values for intercept transit times. When the high-temperature data are plotted against transit time, however, transit-time intercept values of 41 and 22 microseconds result, much lower than the realistic values of 46 and 49 microseconds obtained using the low-temperature data from these wells. These low values are to be expected if porosity values from core analyses are too high because bound water from gypsum was included as porosity.

The plots of transit time versus core porosity for wells 1539 and 1540 gave intercept times of 38 and 42 microseconds which are lower than the values of 46 to 49 microseconds that should result from the mixture of dolomite and anhydrite/gypsum that constitutes this reservoir. Although the core-analysis reports state that low-temperature core-analysis procedures were used, this test suggests that temperatures sufficiently high to drive off the bound water were reached during analysis. Therefore, these core data were not used in the study.

The only useful core data from Section 15 are the results of low-temperature analysis from wells 1535 and 1560. Combining core porosity with transit time for these wells results in the relationship shown in Figure 7 and in equation 4 which was applied for all zones in this study except the CZ zone.

Wells 1535 and 1560 $\phi_c = .99\Delta t - 46.0$ (4)
Cor. = 0.87 Δt intercept = 46.6 μsec

The CZ zone exhibits lower transit times for a given core porosity than other zones. These lower transit-time values can be explained by the presence of only 8 percent anhydrite/gypsum in the CZ zone, whereas the rest of the zones average 15 to 21 percent. Equation 5 was used to calculate porosity in the CZ zone (Fig. 8).

$$\phi_c = 0.76\Delta t - 29.7 \quad (5)$$

There are 33 wells with acoustic logs (mainly Schlumberger Sonic logs) in Section 15. The average porosity of the interval between the M marker and the Y siltstone bed, excluding the siltstone beds, is 8.2 percent. Using a 6-percent porosity cutoff for net pay, the average net-pay porosity is 10.3 percent. The average amount of net pay per well is 121 ft. Zonal averages are given in Table 1. Net values are based only on those intervals within a zone having 6-percent porosity or more, whereas gross values are based on the entire zone.

TABLE 1

POROSITY AND THICKNESS AVERAGES BY ZONE

ZONE	POROSITY (%)		THICKNESS (FT)	
	NET	GROSS	NET	GROSS
YZ	9.1	5.2	3.6	9.6
CZ	11.4	11.3	14.9	15.1
BC	10.0	8.2	27.5	40.9
AB	8.4	6.2	9.1	19.0
MA	10.4	8.6	65.5	94.2

Water Saturation

Water-saturation values are calculated from log analysis using the Archie equation (Archie, 1942).

$$S_w^{-n} = (R_t/R_w)\ \phi^m \qquad (6)$$

Porosity was calculated from the transit-time calibration curves developed previously. The lithologic exponent "m" varies with the amount of vuggy porosity (Lucia, 1983), but since little vuggy porosity exists (Fig. 5) a value of 2.2 was used. The saturation exponent "n" was assumed to be 2. Rock resistivity was read from deep Laterolog curves. Environmental corrections for bore-hole conditions were omitted because few microresistivity logs are available. In some areas, deep and shallow Laterolog resistivity values are approximately equal, indicating that true resistivity of the rock is equal to deep resistivity. In the few wells where microresistivity logs were available, deep resistivity values were corrected for bore-hole conditions using tornado charts (Schlumberger, 1984), and the resulting water-saturation values were compared with those obtained using uncorrected deep resistivity values. As indicated in Table 2, the differences are small and well within the accuracy of the other data used to calculate original oil in place.

TABLE 2

	AVERAGE Sw BY ZONE				NET PAY	SoPhiH
	CZ	BC	AB	MA		
Uncorrected Deep Resistivity	.22	.27	.42	.42	106	7.24
Corrected Deep Resistivity	.19	.25	.36	.40	105	7.48

The resistivity of the formation water was calculated from water samples. A chemical analysis of water produced from well 1515 showed total dissolved solids of 56,526 mg/L in March 1976 before water injection. At the reservoir temperature of 96° F, the resistivity of this water is 0.15 ohm. This value of Rw was verified using the Pickett Plot (Pickett, 1966) and Rxo/Rt plot.

The history of water injection must be considered in order to interpret the calculated water saturations. Water injection in Section 15 started at well 1530 in 1976 and was followed by injection into other wells beginning in 1980. Some wells drilled since 1980 near injectors contain porous zones with high water saturation, indicating the passage of flood water. Also, offset operators started injecting water into the Grayburg between 1969 and 1971 and some of this water could have invaded Section 15, thereby affecting the results of water-saturation calculations. Saturation values from nearby wells were used instead of the values from these porous intervals having abnormally high values of water saturation.

The results of the water-saturation calculations are summarized by zones in Table 3. The difference in water-saturation values is attributed to differences in pore geometry. These differences will be used later to develop a method for determining pore-geometry families for permeability prediction.

TABLE 3

NET-PAY WATER SATURATIONS BY ZONE

ZONE	Sw
YZ	0.52
CZ	0.31
BC	0.43
AB	0.54
MA	0.47
SILTSTONES	1.00

Calculation of Stock-Tank Original Oil in Place

Stock-tank original oil In place was calculated using the volumetric equation. Input data were derived from wells drilled after 1978, some 20 years after initial development. Porosity values have not changed during that time, but water saturation may have changed depending on the reservoir drive mechanism. The Dune field produces by pressure depletion, thus water saturations should not change significantly. Water encroachment has occurred, probably from offset waterflooding operations, but this has been accounted for in the calculation of the water-saturation values. The decrease in pressure has liberated dissolved gas, calculated at 9-percent gas saturation in 1978 (Mobil Oil Corporation, 1978).

A value for porosity times oil saturation times thickness (SoPhiH) was calculated for each well on the basis of a porosity cutoff of 6 percent and/or a resistivity cutoff of 1,000 ohmm. Intervals having less than 6 percent porosity or greater than 1,000 ohmm resistivity were considered to be 100-percent water saturated. These values were posted on maps and contoured using depositional models as guides. SoPhiH maps of the total productive interval from the Y siltstone marker to the M marker, and maps of individual zones, were constructed. Some wells did not penetrate to the M marker, and values for these wells were increased in accordance with the amount of section not

penetrated. The maps were planimetered, and the resulting volumes input into the volumetric equation. A value of 1.128, provided by Mobil Oil Company, was used for B_o.

The results, summarized in Table 4, indicate an original oil in place of 31 million barrels of oil in the Grayburg reservoir in section 15, with 58 percent located in the MA zone and 25 percent in the BC zone. Cumulative production is approximately 11 million barrels, leaving 20 million barrels of oil remaining as of January 1, 1987.

TABLE 4

ORIGINAL OIL IN PLACE
SECTION 15

ZONE	OOIP (MMB)	
YZ	0.98	(3%)
CZ	2.44	(8%)
BC	7.72	(25%)
AB	1.74	(6%)
MA	18.02	(58%)
TOTAL	30.90	(100%)

CUMULATIVE PRODUCTION

Once the original oil in place had been determined, the next step was to determine the volume of oil produced. Cumulative production of oil and water is among the more reliable information normally available from old fields. Although there are usually insufficient pressure data to estimate fluid migration among wells, isoproduction contours can give reasonable insight into the areal distribution of production capacity. Wells used to construct such a map should have similar production histories and exclude waterflood response.

The cumulative production map for Section 15 (Fig. 9) shows a pronounced northwest-southeast trend of high production with the highest production in the southeast quadrant. Depositional facies maps of the MA and the CZ zones show trends of grainstones similar to that of the isoproduction contours. The map is based on production information from wells drilled in the initial development program between 1954 and 1957, and only production data from these wells through December 1980 is included in order to exclude any production in response to waterflooding. However, since waterflooding was initiated in areas bordering Section 15 between 1969 and 1971, some of the production prior to January 1981 may be in response to these bordering waterflooding operations.

Cumulative-production figures show regional depletion of the field, but they provide little insight into pattern (areal recovery) or conformance (vertical recovery) efficiency of the recovery process. Since most wells are completed in

multiple zones and have been pumping most of the time, the stratigraphic distribution of production information on a per-well basis is unavailable from production statistics alone. However, petrophysical and petrographic data obtained from cores and logs provide the additional information required to allocate production stratigraphically and result in three-dimensional geographic displays of the remaining mobile oil in the field. This information is indispensable in planning any supplemental-oil recovery program. Since productivity is related to permeability, knowledge of the permeability distribution in the reservoir can be used to allocate production to various geologic intervals or facies. The next section presents the results of research on methods of obtaining permeability values data from wireline logs.

PERMEABILITY FROM WIRELINE LOGS

Permeability is a fundamental rock property that determines the fluid-flow characteristics of a petroleum reservoir. As such, the amount and distribution of permeability is of paramount importance to understanding the production history and future performance of any hydrocarbon reservoir. Since it can be directly related to productivity, the distribution of permeability in the reservoir can be used to allocate total production to specific geologic units.

Permeability can be determined from measurements made on core material or from pressure-buildup analyses, but cores and pressure-buildup curves are usually rare, especially for old fields. Wireline logs, the most common source of subsurface data, do not measure permeability, but empirical relationships can be established between log response and permeability.

The most common relationship is between porosity and permeability. In carbonate rocks, this relationship is usually very poor due to complex distribution of pore space. Investigators have shown that permeability is related to rock fabric as well as to porosity (Archie, 1952; Lucia, 1983). Therefore, when rock-fabric data are integrated with porosity and permeability data, more precise interrelationships are established.

Determining permeability distribution is best done through knowledge of the depositional and diagenetic processes that produced the rock fabric. Thus, a thorough knowledge of rock fabrics not only improves permeability estimations but also provides the link between engineering parameters and geologic history necessary to describe the engineering parameters in three dimensions.

Rock-Fabric Types

Archie (1952) divided carbonate pore space into matrix and visible porosity and divided visible pore space into sizes. In this study, pore space is divided into interparticle and vuggy on the basis of the relationship of pore space to the

rock fabric (Lucia, 1983). Interparticle porosity includes both intergranular and intercrystalline porosity, whereas vuggy porosity refers to all other types of porosity. Although this is somewhat different from the Choquette and Pray classification (1970), it is in close agreement with general usage in the oil industry.

The Dune field reservoir is composed of intergranular and intercrystalline pore space. Very little vuggy pore space is present. Intergranular pores occur in peloid grainstones between peloid grains that average 180 microns in diameter. Intercrystalline pores are located between dolomite crystals that have replaced wackestones and packstones which contained considerable micrite. The crystals range from less than 20 microns to 80 microns in diameter, but most crystals range from 30 to 80 microns in diameter and average about 50 microns. Most reservoir intervals contain either intercrystalline or intergranular porosity but some intervals contain both types mixed on a scale of inches. Therefore, three "pore families" are recognized: dolomitized grainstones with intergranular pore space, dolomitized wackestones with pore space between 50-micron dolomite crystals, and a mixed fabric with both intergranular and intercrystalline pores, which is commonly described as either a grainstone or a packstone.

Relationships of Porosity, Rock Fabric, and Permeability

Lucia (1983) showed that the permeability of nonvuggy carbonates is related to particle size and interparticle porosity. This relationship, shown in Figure 10, is based on closely controlled laboratory data from a wide variety of carbonate reservoir rocks, and therefore the resulting relationship is considered to be a standard to which other data can be compared.

A similar relationship between particle size, interparticle porosity, and permeability has been established in the Dune field. Figure 11 shows the porosity - permeability - rock-fabric relationship in the Dune field compared with the standard developed by Lucia (1983). Dune reservoir samples with intergranular pore space between 180-micron particles plot close to or within the greater-than-100-micron field of Lucia (1983). Dune field samples with intercrystalline pore space between 50-micron diameter dolomite crystals plot close to or within the 20-to-100-micron field except in the low porosity ranges where the permeability values are too high. Dune reservoir samples with a mixture of intergranular and intercrystalline pore space generally plot on the boundary between the two fields of Lucia except in the low-porosity ranges where again the permeability values are too high.

The low-porosity permeability shift is believed to be due to leakage during routine permeability measurements of low-permeability samples. Therefore, only those samples with more than about 5 millidarcy's (md) permeability are considered to be sufficiently accurate for determining mathematical relationships between porosity and permeability for the three pore families.

Samples from the three pore families plot within the particle-size fields of the standard graph published by Lucia (1983). Therefore, porosity-permeability relationships in the Dune field were constructed to have slopes and intercepts similar to the Lucia standard. The following equations relating porosity and permeability were determined for each pore family using the plot position of the higher permeability samples and the average slope of the appropriate standard field.

$$\text{Intergranular} \quad k = (501.19 \times 10^{6})\phi^{8.00} \qquad (7)$$

$$\text{Mixed} \quad k = (7.3841 \times 10^{6})\phi^{6.7204} \qquad (8)$$

$$\text{Intercrystalline} \quad k = (2.171 \times 10^{6})\phi^{6.5333} \qquad (9)$$

Relationships of Rock Type and Saturation

The three pore families have unique water saturations. A Pickett Plot (Pickett, 1966) for well 1535 shows how the pore families described above are related to water saturation in the Dune field (Fig. 12). The intergranular pore family has the lowest water saturation, the intercrystalline pore family has the highest water saturation, and the mixed intergranular-intercrystalline pore family has intermediate water-saturation values. The following saturation fields define the three pore families.

SATURATION FIELD	PORE FAMILY
< 20% Sw	Intergranular
20% - 25% Sw	Mixed intergranular-Intercrystalline
> 25% Sw	Intercrystalline

The relationship between water saturation and pore families is interpreted to be due to different pore-size distributions characteristic of each pore family. Thin-section examination shows that the intergranular pore family has the largest pore sizes, intercrystalline pore family the smallest pore sizes, and the mixed family intermediate pore sizes. Therefore, connate-water saturation should be highest in the intercrystalline pore family and lowest in the intergranular pore family. This relationship will be true above the transition zone where water saturation is controlled by height above the free-water level and by pore-size distribution. The deepest data point used in this analysis is at a subsea depth of -1167, which is 33 ft above an estimated free-water level at a subsea depth of -1200, which locates the interval studied above the transition zone. Water-saturation values are believed, therefore, to be controlled by pore-size distribution and not by height within the reservoir.

Permeability Calculations

A computer program was written to determine the pore family from saturation relationships and then to calculate permeability from the appropriate porosity - pore-family - permeability relationship. The resulting permeability-

depth profile for well 1560 displays an excellent match with the permeability-depth profile based on core-analysis data (Fig. 13).

Permeability Distribution

Permeability profiles were calculated for all the wells in Section 15 that have acoustic logs and Laterologs. As in original-oil-in-place calculations, porous intervals with anomalously high water saturations were assumed to have been flooded by injection water, and, hence, water saturation values from surrounding wells were used. Maps of the product of permeability and thickness (kh maps) using a cutoff of 6-percent porosity and/or 1000 ohmm were prepared for the total productive interval as well as for each geologic zone. Geometric-mean permeability values were applied. The kh values were increased in proportion to the amount of interval penetrated for those wells that did not penetrate the complete zone.

The cumulative-production map for Section 15 (Fig. 9) shows a pattern similar to the kh map of the total productive interval (Fig. 14). Anomalously low production from the well in the center of the high-kh area reflects temporary abandonment in 1971 due to high water cut.

Permeability-feet maps of the geologic zones are summarized in Table 5. Zone AB has a kh of less than 1 md-ft, and it separates the reservoir vertically into the middle and upper geologic units. Zones ZY, CZ, and BC are in the upper geologic unit. Zone ZY exhibits a kh of less than 1 md-ft and only reaches reservoir status in the southern part of the section where values increase to 10 md-ft. Zone CZ contains several areas with kh values up to 500 md-feet (Fig. 15). These areas are elongate northwest-southeast and are controlled by the depositional pattern of pellet grainstone bars. Zone BC has a relatively uniform kh of between 10 and 50 md-ft over most of Section 15 with decreasing values in the northeast quadrant. The MA zone coincides with the middle geologic unit and contains the highest kh values, over 1000 md-feet. High kh values are concentrated in a narrow band trending northwest-southeast through the center of Section 15 and are highest in the southeast quarter of Section 15 (Fig. 16). This trend is believed to represent a local area of abundant grain-dominated packstones and grainstones.

TABLE 5

SUMMARY OF ZONAL KH DATA

ZONE	AVERAGE KH
ZY	0.1
CZ	24.4
BC	11.0
AB	0.5
MA	22.0

DISTRIBUTION OF REMAINING MOBILE OIL

Remaining mobile oil is calculated by subtracting produced oil and residual oil from the original oil in place. Water saturation and residual- oil saturation, as well as the STOOIP and the cumulative production, are critical in determining remaining mobile oil. For the Dune field, Galloway and others (1983) noted a water-saturation value of 25 percent and a residual-oil-saturation value of 30 percent. This study resulted in a much lower value for water saturation, but no attempt was made to determine a residual-oil-saturation value. Since the 25 percent water saturation value was not applied in this report, the 30-percent residual-oil saturation value was not applied. Instead, a residual value equal to one-third of the STOOIP is applied based on common industry practice.

As of January 1981, 7.5 mmbbls of oil had been produced from section 15. Assuming a residual-oil value of one-third the STOOIP, about 13.7 mmbbls of mobile oil remain in the reservoir. Approximately 3.5 mmbbls of oil was produced between 1981 and January 1987, leaving 10.2 mmbbls of mobile oil remaining.

Mapping the distribution of remaining mobile oil required relating the original oil in place and produced volumes to a stratigraphic framework. Geologic zonation and depositional history have been used to map the original oil in place. The first step in relating hydrocarbon volumes that were produced to the stratigraphic framework is to determine the vertical production profile. Because only per-well production data are available, production volumes were allocated to individual geologic zones based on kh. Production data from the initial development wells were used for this allocation. Neither permeability nor SoPhiH values can be calculated from wireline logs from these initial wells because the wells were drilled before the development of the acoustic-logging technique. Permeability and SoPhiH values for these initial wells were taken from the permeability-feet and SoPhiH isopach maps produced using data from wells drilled during 197- to 1986. Values for permeability-feet were obtained for each zone in each initial well based on the isopach maps, and the production values from each initial well were allocated to each zone according to the fraction of the total permeability-feet in each zone. Similarly, SoPhiH values for the initial wells were taken from the SoPhiH isopach maps for each zone and used to calculate oil in place, assuming 20-acre drainage.

Remaining mobile oil for each reservoir zone in Section 15 was calculated by subtracting produced oil and the residual oil from the original oil in place. The results are shown in Table 6. Thirty-eight percent of the total oil produced from Section 15 came from the CZ zone even through the zone contained only 8 percent of the original oil in place. This high productivity is due to the high average permeability for the CZ zone. Only 225,000 barrels of mobile oil remain in the CZ zone in Section 15. Forty-two percent of the total oil produced came from the MA zone that originally contained 58 percent of the original oil in place. As a result, the MA zone contains by far the largest volume of remaining mobile oil: 9,312,000 barrels or 68 percent. The BC zone contains 3,286,000 barrels of remaining mobile oil (24 percent). Little oil has been

recovered from the AB zone, resulting in 886,000 barrels of remaining mobile oil, which is not considered a significant target because the zone has low permeability.

TABLE 6

ZONE	OOIP		PRODUCED OIL		REMAINING MOBILE OIL	
	MMB		MMB		MMB	
CZ	4.4	(15%)	2.9	(38%)	0.2	(2%)
BC	6.7	(22%)	1.4	(19%)	3.3	(24%)
AB	1.5	(4%)	0.1	(1%)	0.9	(6%)
MA	17.8	(59%)	3.1	(42%)	9.3	(68%)
TOTAL	30.4		7.5		13.7	

Maps of remaining mobile oil in each zone in Section 15 as of January 1, 1981 were constructed. The CZ zone (Fig. 17) contains no remaining mobile oil in several areas on the north, east, and south edges of Section 15. Offset operators have been injecting water into the Grayburg reservoir since 1970, evidence that the zone probably has been flooded in these areas. In addition, Mobil has been injecting water into well 1531 since 1976, and log analysis and production performance indicate that by 1981 the CZ zone was flooded in the vicinity of this well.

The MA zone (Fig. 18) contains the largest volume of mobile oil, which is concentrated in a northwest-southeast trend across Section 15. Studies of water-production history suggest that some of the oil produced from the southern tier of wells in Section 15 was in response to water injection by offset operators.

CONCLUSIONS

The maps of remaining mobile oil are indispensable in planning strategies for additional recovery and reserve growth. Careful compilation of these maps enables the planning of suitable infill drilling and well-completion programs and the effective design of flood patterns and, in general, assists in optimum management of any future development program for either remaining mobile or residual oil. Preparation of remaining-oil maps requires the integration of geological, petrophysical, and production data which leads to an understanding of the fluid mechanics of the reservoir. Essential to this integration is an understanding of the detailed geologic setting of the field. In the Dune field, knowledge of the geologic framework permitted the delineation and mapping of reservoir zones. Facies were mapped within each zone to produce a three-dimensional view of the overall depositional fabric, which relates directly to cumulative production trends.

Rock-fabric data and mineralogy have been related to wireline-log response in order to transform transit-time and resistivity values into porosity, permeability,

and water saturation values. The Dune field contains up to 55 percent gypsum, causing neutron and density logs to indicate anomalously high porosity values. Acoustic logs are not as responsive to gypsum but are responsive to vuggy porosity. However, vuggy porosity was determined to be very low in these reservoir rocks. Therefore, an excellent calibration of acoustic logs with porosity values derived from low-temperature core analyses was obtained. Water-saturation values were calculated using porosity values taken from acoustic logs and resistivity values from deep-focused resistivity logs.

Three pore-geometry families were identified on the basis of rock-fabric studies: intergranular porosity in dolomitized grainstones, intercrystalline porosity in dolomitized wackestones, and a mixed intergranular and intercrystalline porosity in dolomitized packstones. A porosity-permeability transform function was derived for each pore-geometry family. Each family displays a unique water-saturation field on porosity-resistivity cross plots. Thus, permeability can be calculated from velocity and resistivity logs using permeability transform functions. Permeability values and vertical profiles calculated by this method are significantly more realistic than those calculated by methods that assume a uniform rock fabric.

Cumulative-production statistics are available for each well in Section 15. The wells are typically completed in all zones, and few individual zone tests are available. To map the distribution of the remaining mobile oil, well production values must be allocated to geologic zones. This was accomplished in this study by calculating permeability-feet values for each zone in each well and allocating the well production values according to the proportion of permeability-feet.

Geological, petrophysical, and production studies were integrated to produce the maps of mobile oil. The volume of mobile oil through 1980 was calculated for each zone in each well by subtracting zonal production and residual oil from the original oil in place for that zone for 20 acres around that well. Contour maps of this data show that most of the remaining mobile oil occurs in areas with the highest cumulative production. These areas have the highest permeability-feet and greatest original oil in place, and their locations are controlled by the distribution of grain-dominated sediments. The MA zone is calculated to contain 9.3 million barrels of oil, 68 percent of the remaining mobile oil as of 1981. Most of the conventionally recoverable oil occurs in a narrow northwest-southeast trend and is concentrated in the southeast quarter of Section 15. An infill-drilling and recompletion strategy in the MA zone based on the distribution of remaining mobile oil should result in a significant increase in oil recovery.

ACKNOWLEDGMENTS

Major funding for the research was provided by The University of Texas System and strong support was provided by geologists and engineers of Mobil Producing Texas and New Mexico, Inc. Technical assistance was provided by geology students K. L. Herrington and D. A. Leary and by engineering students M. H. Holtz, M. G. Lewis, and S. H. Schmidt. C. M. Garrett, Jr., Bureau of Economic Geology, and the staff of the University Lands Office in Midland provided reserve, production, and well information throughout the project.

REFERENCES

Archie, G. E., 1942, The electrical resistivity log as an aid in determining some reservoir characteristics: Trans., American Institute of Mining, Metallurgical and Petroleum Engineers, v. 146, p. 54-62.

_____ 1952, Classification of carbonate reservoir rocks and petrophysical considerations: American Association of Petroleum Geologists Bull., v. 36, no. 6, p. 278-298.

Bebout, D. G., Lucia, F. Jerry, Hocott, C. R., Fogg, G. E., and Vander Stoep, G. W., 1987, Characterization of the Grayburg reservoir, University Lands Dune field, Crane County, Texas: University of Texas at Austin, Bureau of Economic Geology Report of Investigations No. 168, 98p.

Choquette, P. W., and Pray, L. C., 1970, Geologic nomenclature and classification of porosity in sedimentary carbonates: American Association of Petroleum Geologists Bull., v. 54, p. 207-250.

Galloway, W. E., Ewing, T. E., Garrett, C. M., Tyler, N. and Bebout, D. G., 1983, Atlas of major Texas oil reservoirs: University of Texas at Austin, Bureau of Economic Geology Special Publication, 139p.

Lucia, F. J., 1983, Petrophysical parameters estimated from visual description of carbonate rocks: a field classification of carbonate pore space: Journal of Petroleum Technology, March, p. 629-637.

Mobil Oil Corporation, 1978, Application for optional 10-acre spacing, Dune field, Crane County, Texas: Railroad Commission of Texas Hearing, Case No. 8-68323, February 2, 1978.

Pickett, G. R., 1966, A review of current techniques for determination of water saturation from logs: Journal of Petroleum Technology, November, p. 1425-1433.

Pirson, S. J., 1983, Geologic well log analysis: Houston, Texas, Gulf Publishing Company, 475 p.

Schlumberger, 1972, Log interpretation, Volume I -- Principles: Schlumberger Limited, p. 85.

----------, 1984, Log interpretation charts: Schlumberger Limited, p. 74.

Tilly, H. P., Gallagher, B. J., and Taylor, T. D., 1981, Methods for correcting porosity data in a gypsum bearing carbonate reservoir: Permian Basin Oil and Gas Recovery Symposium, Society of Petroleum Engineers Preprint no. 9716.

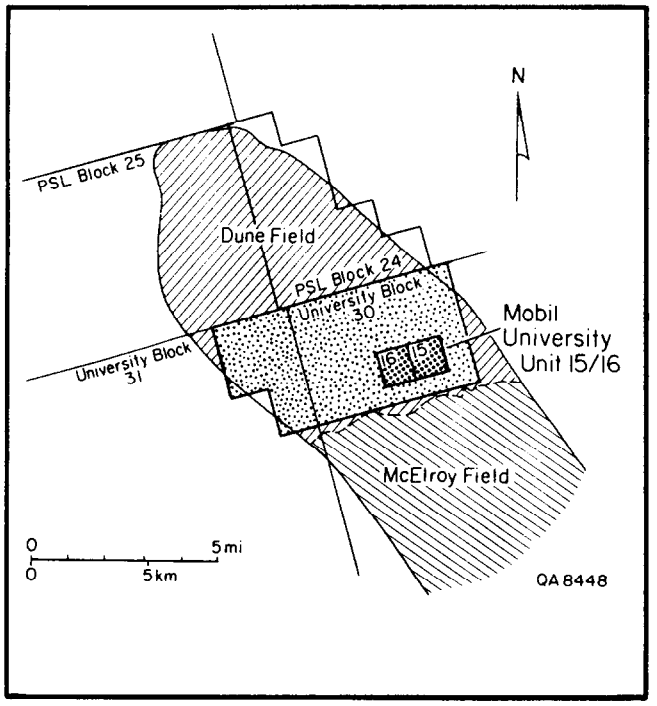

Figure 1 - Map of the Dune field and the northern end of the McElroy field, showing the location of University Blocks 30 and 31, the Dune field study area, and Mobil University Unit 15/16

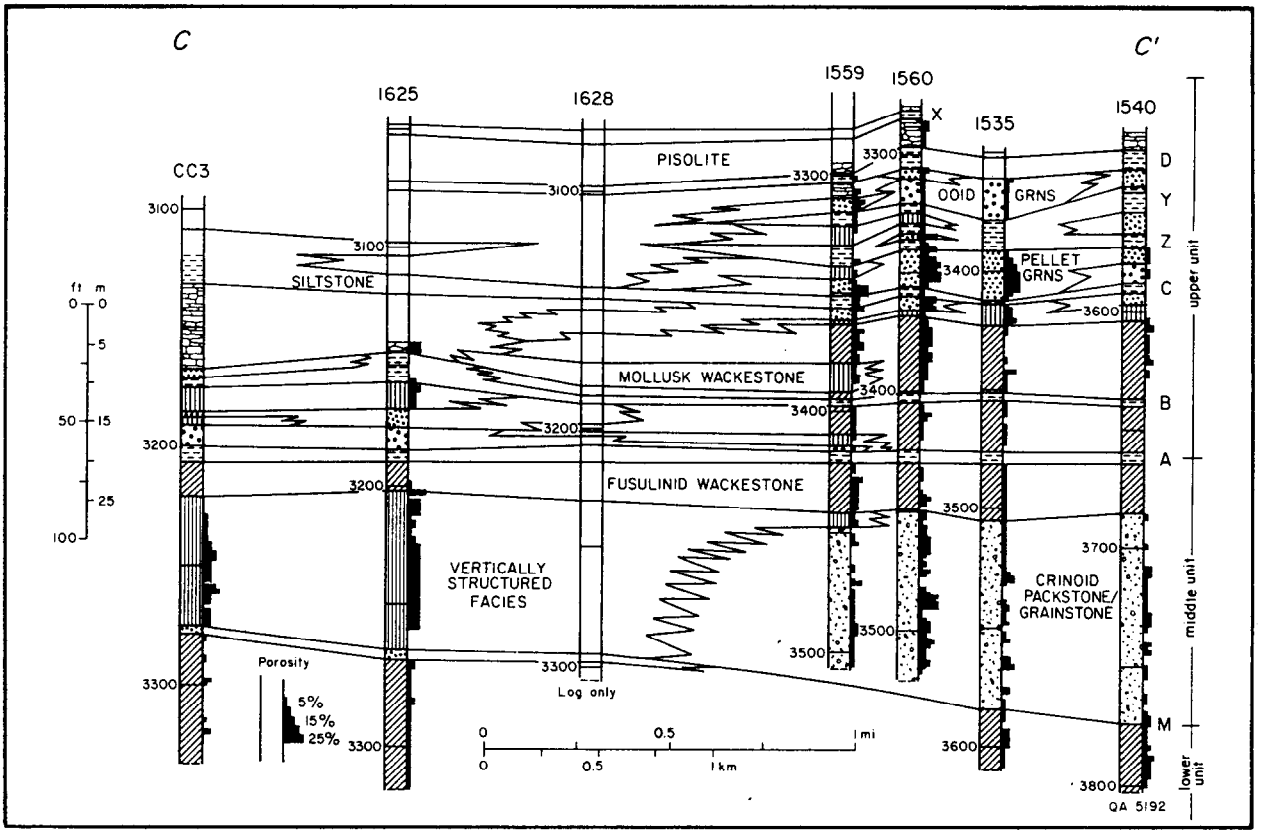

Figure 2 - Facies dip section C-C' across the Dune field — location of the cross section is shown as P-P' in Figure 3

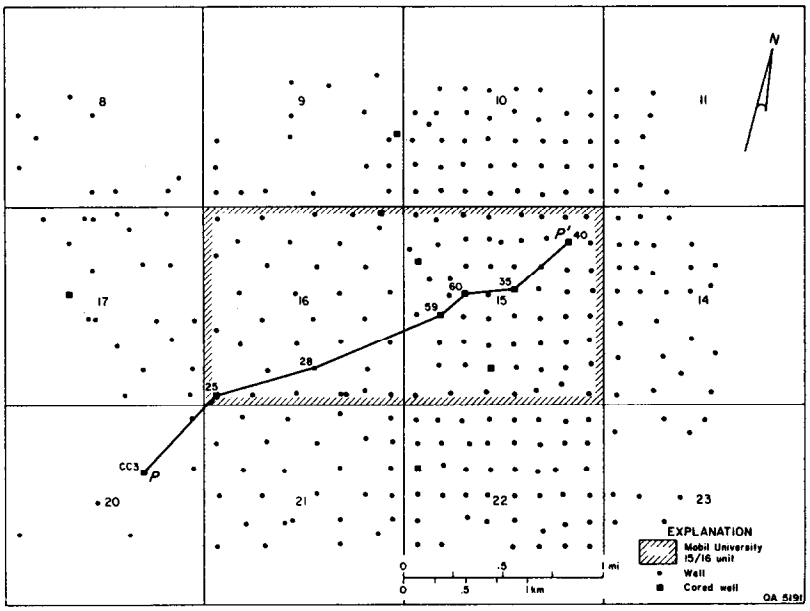

Figure 3 - Well control in the Mobil University Unit 15/16 and neighboring area — location of the P-P' cross section, shown as C-C' in Figure 2, is also shown

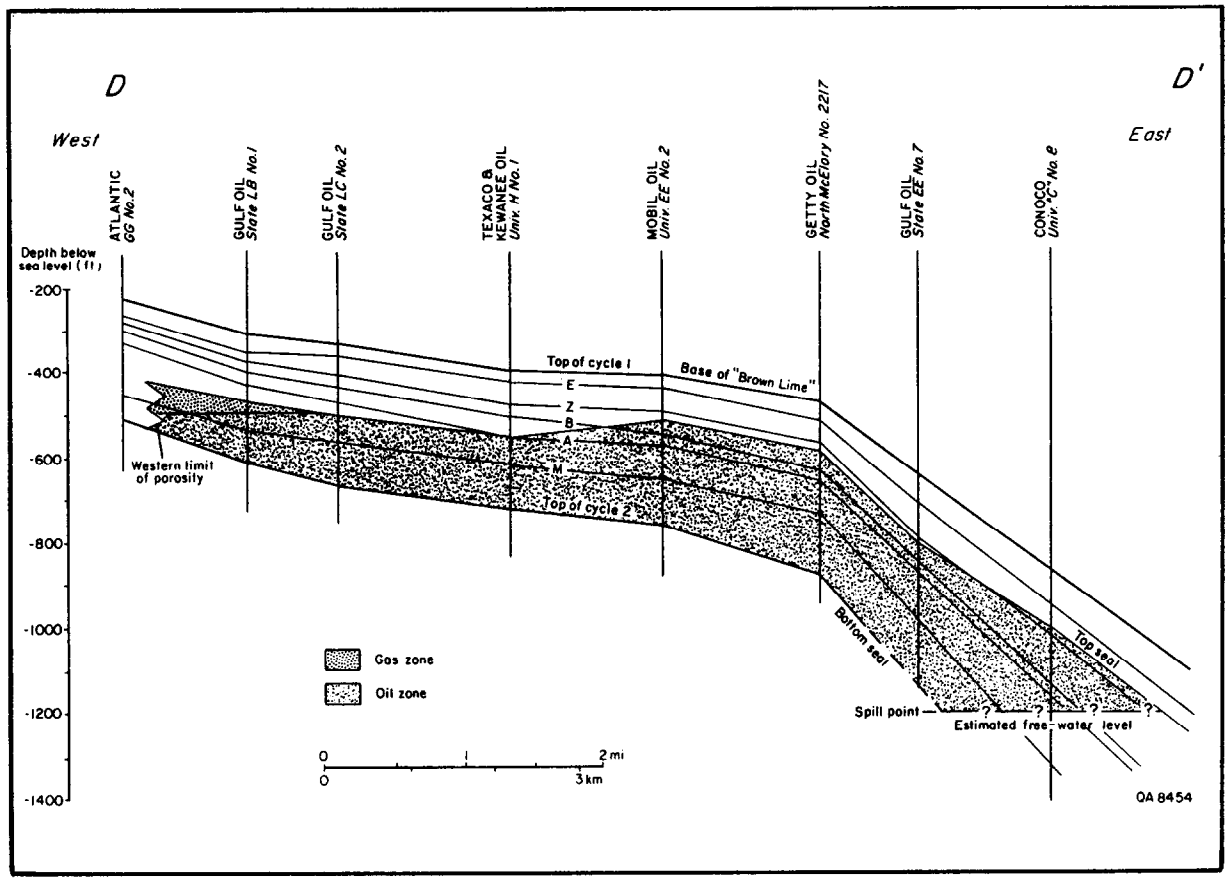

Figure 4 - West-to-east structural section across the Dune field showing the correlation of the major siltstone markers, the top seal of the reservoir, the oil-producing zone, the bottom seal, and the free-water level

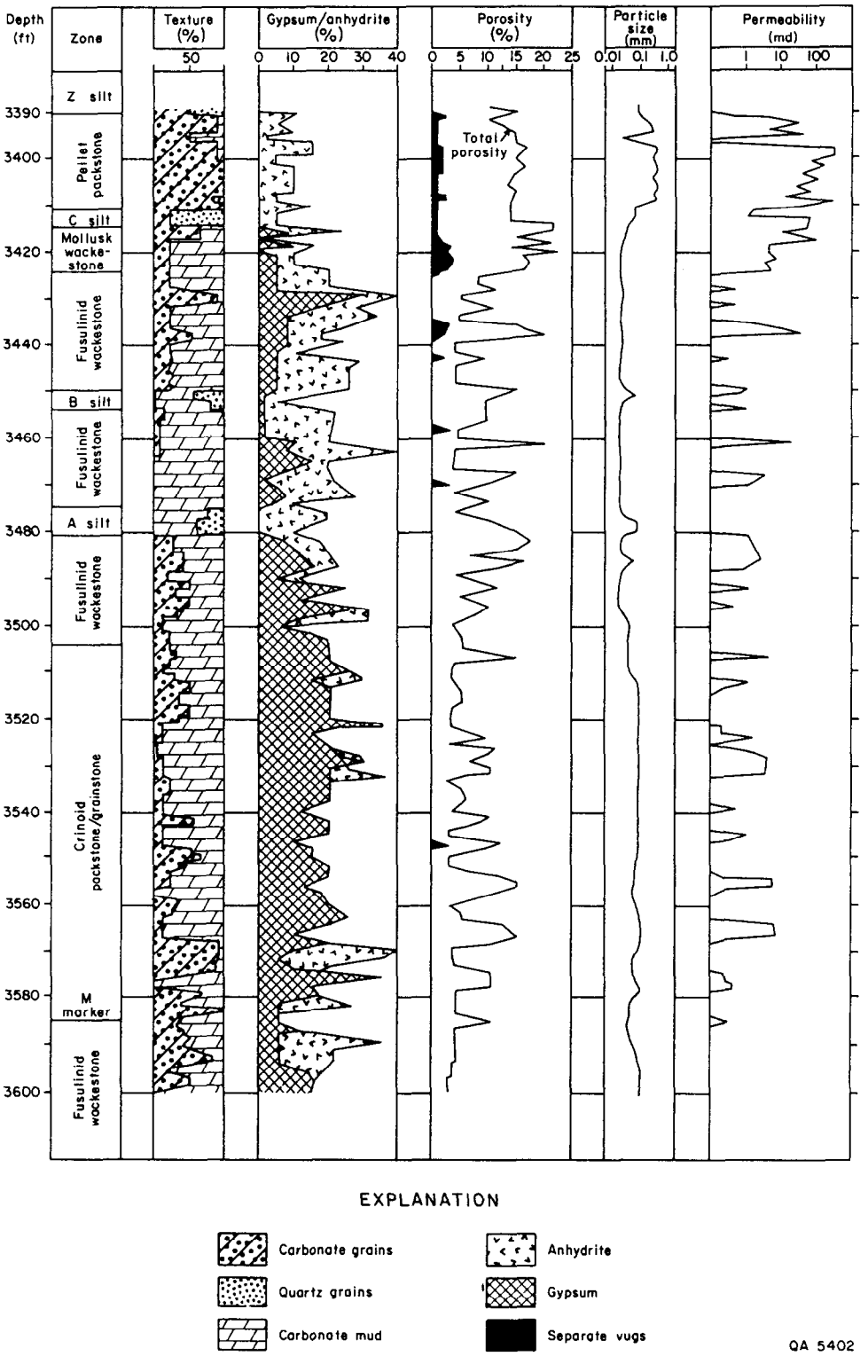

Figure 5 - Comparison of textural and mineralogical properties determined from point-counting thin sections with porosity and permeability analyzed from core from Mobil University 1535

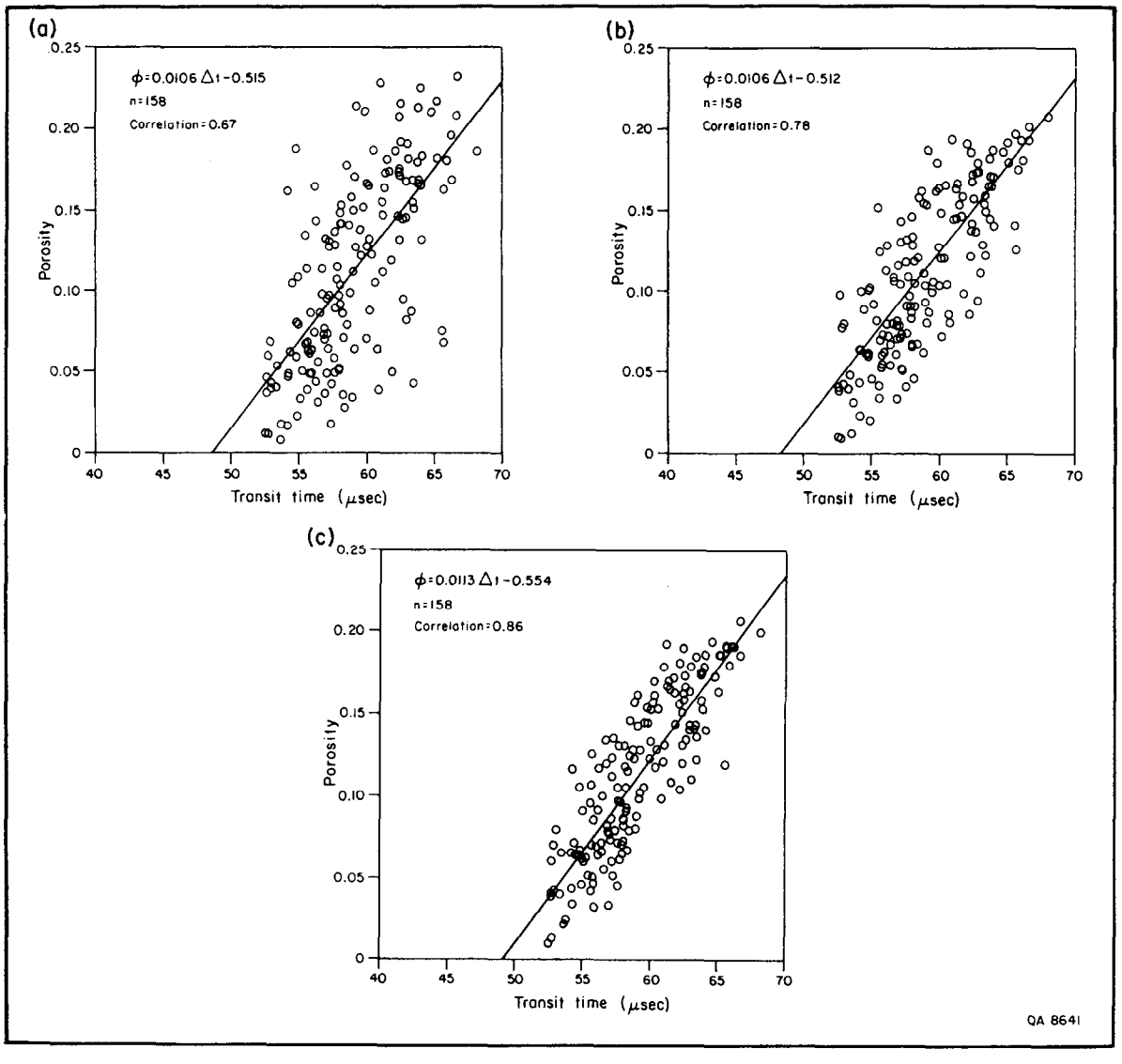

Figure 6 - Effect of depth adjustments and averaging on the transit-time-porosity relationship in Mobil University 1560: (a) using core gamma-ray and well gamma-ray logs for depth adjustment; (b) adding 3-ft averaging of core porosities to (a); and (c) adding depth adjustments using peak porosities and transit times to (b)

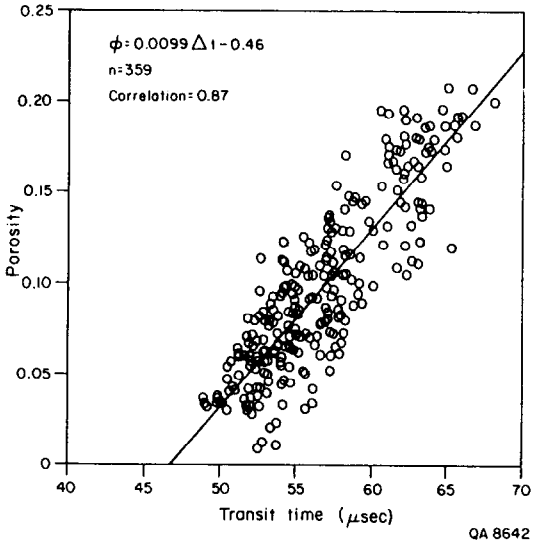

Figure 7 - Acoustic transit time, porosity, and transform function for the interval from the M marker to the C marker in Mobil University 1535 and 1560

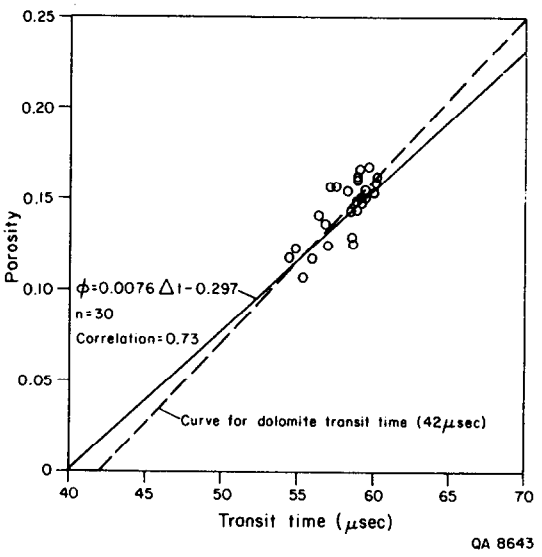

Figure 8 - Acoustic transit time, porosity, and transform function for the CZ zone in Mobil University 1535 and 1560

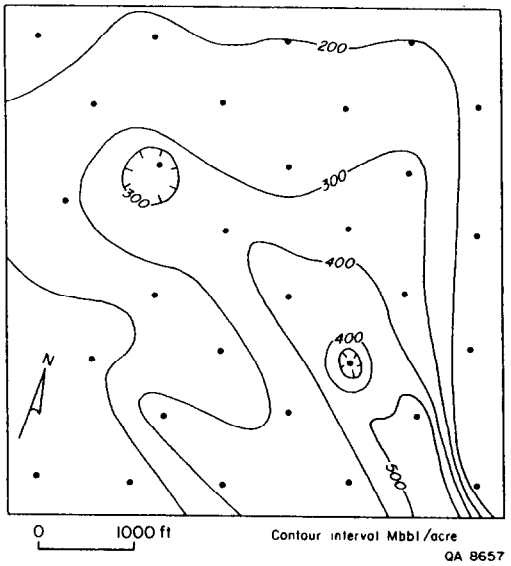

Figure 9 - Isoproduction map for Section 15, Dune field, showing distribution of cumulative production from initial development wells in January 1981

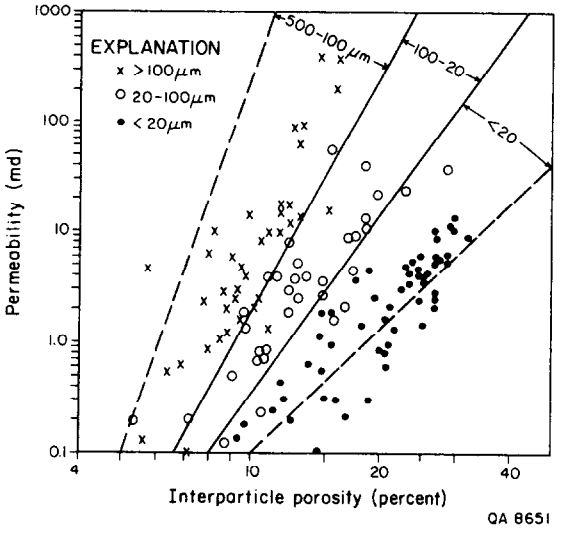

Figure 10 - Porosity-permeability cross plot for various particle-size groups in nonvuggy carbonate rocks (Lucia, 1983)

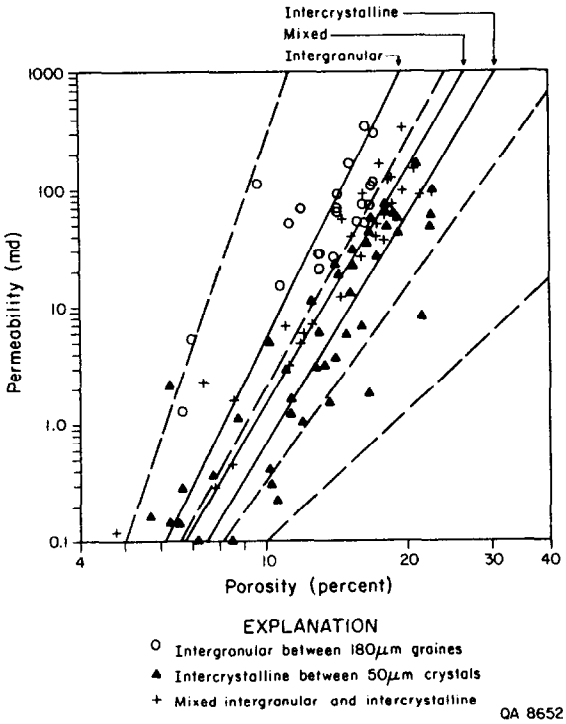

Figure 11 - Porosity-permeability cross plot for the three pore families recognized in the Dune field — the particle-size fields from Lucia (1983) are shown in dashed lines for comparison

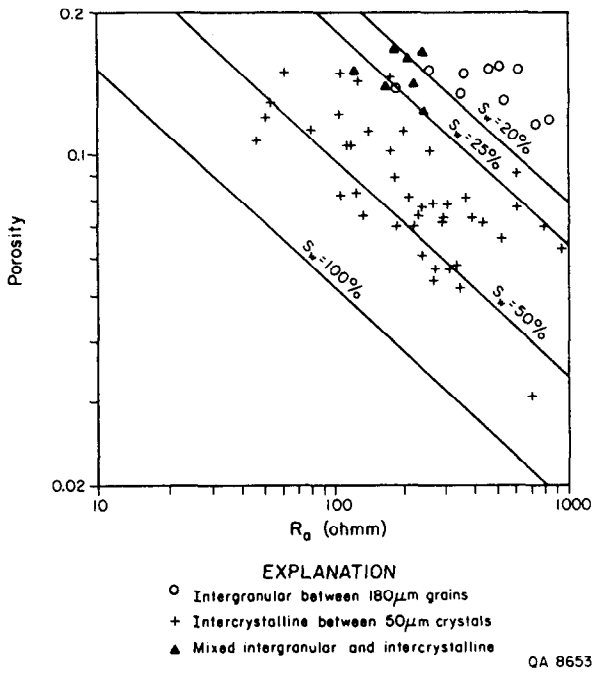

Figure 12 - Pickett Plot for Mobil University 1535 showing the relationship between water saturation and pore families

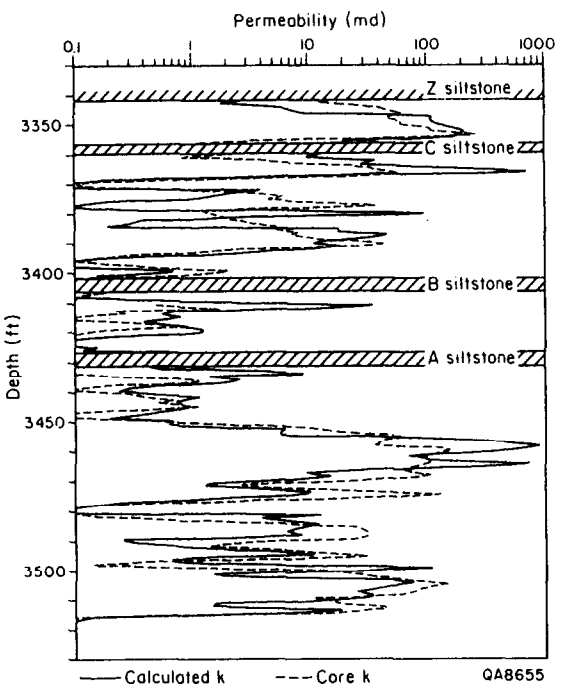

Figure 13 - Depth plot for Mobil University 1560 comparing core permeability with permeability calculated from rock-fabric transform functions

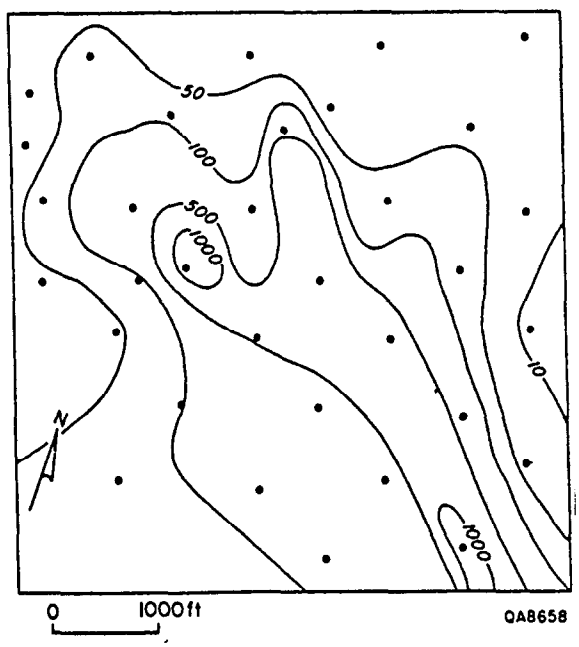

Figure 14 - Isopach map of net permeability-feet in the Grayburg reservoir, Section 15, Dune field

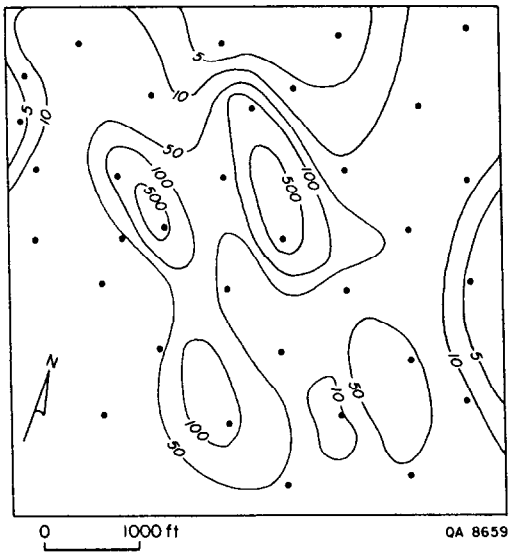

Figure 15 - Net-kh map of the CZ zone, Section 15, Dune field — the elongated trend of the high values corresponds to the position of pellet grainstone bars

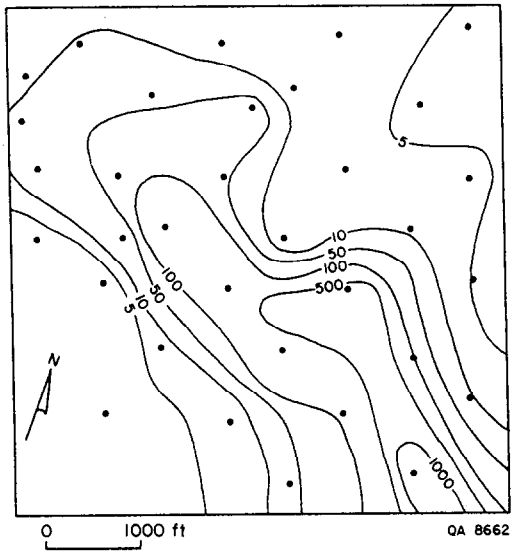

Figure 16 - Net-kh map of the MA zone, Section 15, Dune field — the elongated trend of the high values corresponds to the position of composite grainstone bars

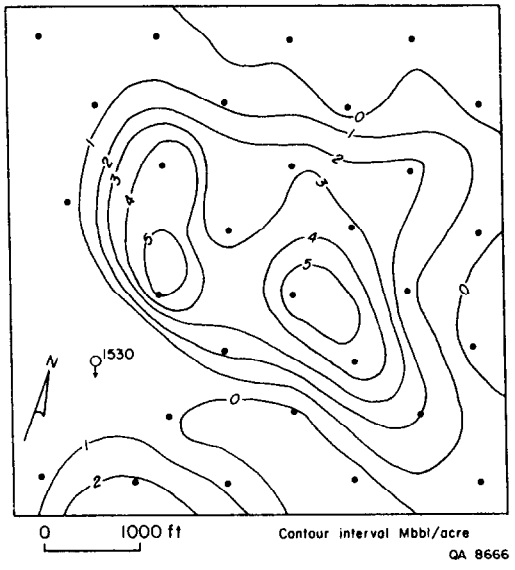

Figure 17 - Map showing distribution of remaining mobile oil in the CZ zone, Section 15, Dune field, in January 1981

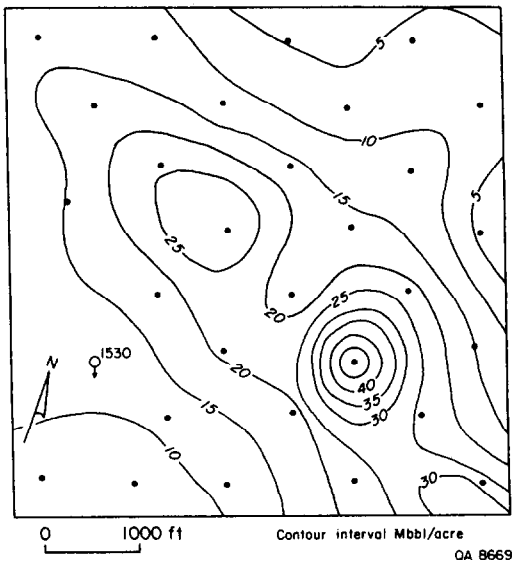

Figure 18 - Map showing distribution of remaining mobile oil in the MA zone, Section 15, Dune field, in January 1981